

# Turbulence and far-from-equilibrium equation of state of Bogoliubov waves in Bose-Einstein Condensates

Ying Zhu,<sup>1,\*</sup> Giorgio Krstulovic,<sup>2</sup> and Sergey Nazarenko<sup>1</sup>

<sup>1</sup> *Université Côte d'Azur, CNRS, Institut de Physique de Nice (INPHYNI), 17 rue Julien Lauprêtre, 06200 Nice, France*

<sup>2</sup> *Université Côte d'Azur, Observatoire de la Côte d'Azur, CNRS, Laboratoire Lagrange, Boulevard de l'Observatoire CS 34229 – F 06304 Nice Cedex 4, France<sup>†</sup>*

Bogoliubov waves are fundamental excitations of Bose-Einstein Condensates (BECs). They emerge from a perturbed ground state and interact nonlinearly, triggering turbulent cascades. Here, we study turbulent BECs theoretically and numerically using the 3D Gross-Pitaevskii model and its wave-kinetic equations. We derive a new Kolmogorov-like stationary spectrum for short Bogoliubov waves and find a complete analytical expression for the spectrum in the long acoustic regime. We then use our predictions to explain the BEC equation of state reported in [*Dora et al. Nature* **620**,521 (2023)], and to suggest new experimental settings.

Turbulence, in the broad sense, is perhaps one of the most striking manifestations of far-from-equilibrium physics in Nature. In classical fluids, it emerges when the forcing scale, at which energy is injected, is well-separated from the one at which it is dissipated by molecular viscosity. Energy is then carried along scales through a turbulent cascade driven by hydrodynamic interactions. An analogous process occurs in nonlinear wave systems, where cascades are driven by the interaction of waves having different wavelengths. When the wave nonlinearity is weak, the Wave Turbulence Theory (WTT) provides a comprehensive theoretical framework describing far-from-equilibrium steady-states [1]. The theory has been successful in describing, for instance, the dynamics of gravitational waves [2], Kelvin waves on superfluid vortices [3], internal gravity waves in the ocean [4, 5], Langmuir waves in plasmas [6], and matter waves in turbulent Bose-Einstein Condensates (BECs) [7, 8].

One of the most interesting and important regimes in BEC turbulence is realized when weak waves propagate on a background of a coherent ground state, the condensate. These are the Bogoliubov waves, whose frequency  $\omega$  in the linear approximation is given by the following dispersion relation,

$$\omega_k \equiv \omega(k) = c_s k \sqrt{1 + (k\xi)^2/2}, \quad (1)$$

where  $k = |\mathbf{k}|$  is the modulus of the wave vector  $\mathbf{k}$ ,  $c_s$  is the speed of sound, and  $\xi$  is the healing length of the BEC at which dispersive effects become important. In the absence of vortices, and with a strong condensate, the leading nonlinearity is quadratic, and wave interactions involve only three waves. When the condensate is negligible, the interaction term is cubic and the relevant nonlinear processes are 4-wave interactions. Over the last few years, outstanding progress has been achieved in realizing turbulent BECs experimentally, and they have become an excellent prototype for studying far-from-equilibrium physics.

Turbulent states are driven by external forcing and dissipation, which results in an energy flux  $P_0$  through scales (which equals the energy injection and dissipation rates). Such fluxes thus play a role equivalent to the one of temperature in equilibrium thermal states. It is then natural to ask if there is a universal far-from-equilibrium equation of state (EoS) relating energy flux and internal observables, such as the energy or the wave-action spectrum. The clean and well-controlled turbulent BEC experiments available today [9], together with recent numerical simulations of the Gross-Pitaevskii equation [10], have led to revealing the existence of such EoS. They have shown that the amplitude of the wave-action spectrum scales with the flux as  $P_0^{1/3}$ , followed by a  $P_0^{2/3}$ -scaling for large flux. Whereas the  $P_0^{1/3}$ -scaling can be understood within the WTT invoking 4-wave interactions, the second scaling-law lacks explanation. Also, data uncertainties do not uniquely fix the exponents.

In this Letter, we will revise old and obtain new theoretical predictions for the BEC turbulence dominated by interacting Bogoliubov waves. We test these predictions by numerical simulations and use our results to provide a plausible theoretical explanation of the second scaling law of the EoS observed in BEC turbulence. In particular, we argue that it is consistent with scaling  $P_0^{1/2}$  arising from interacting short-wave Bogoliubov modes. We re-analyze the experimental data of [9], and show their agreement with our prediction.

The master model for describing BECs is the Gross-Pitaevskii equation (GPE) for the complex scalar wave function  $\Psi(\mathbf{x}, t)$ , where  $\mathbf{x}$  is the position in 3D physical space and  $t$  is time. Defining  $\Psi$  such that  $|\Psi|^2$  is the mass density, the GPE written in terms of  $\xi$ ,  $c_s$ , and the unperturbed (uniform) condensate mass density  $\rho_0$ , reads

$$i \frac{\partial \Psi}{\partial t} = \frac{c_s}{\sqrt{2}\xi} \left[ -\xi^2 \nabla^2 + \frac{|\Psi|^2}{\rho_0} - 1 \right] \Psi + i F(\mathbf{x}, t) + i \frac{\nabla^{2\alpha} \Psi}{k_R^{2\alpha}}. \quad (2)$$

We have also included a large-scale forcing  $F$  and a hyper-viscous dissipation term acting on small scales, both necessary for describing turbulent states. The heal-

\* ying.zhu@univ-cotedazur.fr

† krstulovic@oca.eu

ing length and the speed of sound depend both on the physical properties of the BEC and  $\rho_0$ .

The GPE can be mapped to an effective compressible irrotational fluid flow via the so-called Madelung transformation,  $\Psi(\mathbf{x}, t) = \sqrt{\rho(\mathbf{x}, t)} \exp[i\phi(\mathbf{x}, t)/\sqrt{2}c_s\xi]$  with  $\rho(\mathbf{x}, t)$  and  $\phi(\mathbf{x}, t)$  being the fluid mass density and the velocity potential, respectively. The Bogoliubov dispersion relation (1) is obtained by linearizing the GPE (2), in the absence of forcing and dissipation terms, considering perturbations over the ground state,  $\tilde{\Psi} = \Psi - \sqrt{\rho_0}$  and diagonalizing them in Fourier space. For weakly nonlinear waves, the leading order interaction occurs between the modes satisfying three-wave resonant conditions,

$$\omega_k = \omega_{k_1} + \omega_{k_2}, \quad \mathbf{k} = \mathbf{k}_1 + \mathbf{k}_2. \quad (3)$$

In this limit, the WTT provides a wave-kinetic equation (WKE) describing the evolution of the wave-action spectrum  $n_{\mathbf{k}} = n(\mathbf{k}, t)$ . The general WKE for weakly nonlinear waves driven by three-wave resonant interactions is [1, 11]

$$\frac{\partial n_{\mathbf{k}}}{\partial t} = \text{St}_{\mathbf{k}}, \quad (4)$$

with the wave-collision integral

$$\begin{aligned} \text{St}_{\mathbf{k}} &= 2\pi \int (\mathcal{R}_{12}^{\mathbf{k}} - \mathcal{R}_{k_2}^1 - \mathcal{R}_{k_1}^2) d\mathbf{k}_1 d\mathbf{k}_2, \\ \mathcal{R}_{12}^{\mathbf{k}} &= \delta_{12}^{\mathbf{k}} \delta(\omega_{12}^k) |V_{12}^k|^2 [n_{\mathbf{k}_1} n_{\mathbf{k}_2} - n_{\mathbf{k}} n_{\mathbf{k}_1} - n_{\mathbf{k}} n_{\mathbf{k}_2}], \quad (5) \\ \delta_{12}^{\mathbf{k}} &= \delta(\mathbf{k} - \mathbf{k}_1 - \mathbf{k}_2), \\ \delta(\omega_{12}^k) &= \delta(\omega_k - \omega_{k_1} - \omega_{k_2}), \end{aligned}$$

where  $V_{12}^k \equiv V(k, k_1, k_2)$  is the three-wave interaction amplitude depending on the particular type of waves. For Bogoliubov waves, they are given by

$$\begin{aligned} V_{23}^1 &= V_0 \sqrt{k_1 k_2 k_3} W_{23}^1, \quad V_0 = \frac{3\sqrt{c_s}}{4\sqrt{2}}, \\ W_{23}^1 &= \frac{1}{2\sqrt{\eta_1 \eta_2 \eta_3}} + \frac{\sqrt{\eta_1 \eta_2 \eta_3}}{6k_1 k_2 k_3} \left( \frac{k_1^3}{\eta_1} - \frac{k_2^3}{\eta_2} - \frac{k_3^3}{\eta_3} \right), \quad (6) \end{aligned}$$

where  $\eta_i \equiv \eta(k_i) = \sqrt{1 + (k_i \xi)^2/2}$  for  $i = 1, 2, 3$ . The Bogoliubov WKE (6) was first derived in [7] in a slightly different form with mistakes in the prefactor. Finally, by assuming isotropy and performing angle average, the WKE becomes

$$\begin{aligned} \frac{\partial n_k}{\partial t} &= \text{St}_k = 4\pi^2 V_0^2 \int_{k_1, k_2 \geq 0} (|W_{12}^k|^2 \mathcal{T}_{12}^k \delta(\omega_{12}^k) \\ &- |W_{k_2}^1|^2 \mathcal{T}_{k_2}^1 \delta(\omega_{k_2}^1) - |W_{k_1}^2|^2 \mathcal{T}_{k_1}^2 \delta(\omega_{k_1}^2)) k_1^2 k_2^2 dk_1 dk_2, \quad (7) \end{aligned}$$

where  $\mathcal{T}_{12}^k = n_{k_1} n_{k_2} - n_k n_{k_1} - n_k n_{k_2}$ . In Appendix A, a revised, rigorous derivation of the WKE, its asymptotic regimes, and the parametrization of the resonant manifold can be found.

In this Letter, we obtain new theoretical predictions for the 3D Bogoliubov WTT in both large- and small-scale

limits. We test these predictions by performing numerical simulations of the GPE (2) and the isotropic WKE (7).

In the large-scale limit  $k\xi \rightarrow 0$ , we have  $\eta_i \rightarrow 1$  and therefore  $\omega_{k_i} = c_s k_i$  – this is the acoustic wave limit. Also, on the resonant manifold we have  $W_{23}^1 \rightarrow 1$ , and thus  $V_{23}^1 \rightarrow V_0 \sqrt{k_1 k_2 k_3}$ , consistently with the result in [12]. The collisional integral of the WKE (7) becomes as in the 3D acoustic WKE [13],

$$\text{St}_k = \frac{4\pi^2 V_0^2}{c_s} \int_{k_1, k_2 \geq 0} (\mathcal{T}_{12}^k \delta_{12}^k - \mathcal{T}_{k_2}^1 \delta_{k_2}^1 - \mathcal{T}_{k_1}^2 \delta_{k_1}^2) k_1^2 k_2^2 dk_1 dk_2, \quad (8)$$

where  $\delta_{12}^k = \delta(k - k_1 - k_2)$ .

Reference [13] obtained a Kolmogorov-type stationary solution for the energy spectrum of 3D acoustic waves:  $E(k) = 4\pi k^2 \omega_k n_k = C_1 c_s^{1/2} P_0^{1/2} k^{-3/2}$ , the so-called Zakharov-Sagdeev (ZS) spectrum. Here, the energy flux is defined as  $P(k) = -\int_0^k 4\pi q^2 \omega(q) \text{St}(q) dq$ , which is constant due to the spectrum's stationarity,  $P = P_0 = \text{const}$ . An approximation of the dimensionless constant  $C_1$  was given in [13], as well in a recent paper [14]. We derive its exact analytical expression in Appendix B. The complete ZS spectrum reads:

$$E(k) = C_1 c_s^{1/2} P_0^{1/2} k^{-3/2}, \quad C_1 = 1/\sqrt{3\pi(\pi + 4 \ln 2 - 1)}. \quad (9)$$

Note that the acoustic WKE (8) is derived as an asymptotic limit of (7). Unlike the 2D case where  $\text{St}_k \propto \xi^{-1}$  [12], in 3D,  $\xi$  cancels out after angle averaging [11] leading to (8). However, in practice, a small amount of dispersion is still crucial in the system to regularize the wave dynamics and avoid singularities. Note that in the recent work [14], the authors numerically obtained the ZS spectra in 3D acoustic wave systems, and different values of constant were reported for the dispersive and non-dispersive cases. In Appendix A and B, we show that the WKE of non-dispersive acoustic waves is regular for the 3D isotropic case, but with a different prefactor. Consequently, the ZS spectrum comes with a different constant.

In the small-scale limit  $k\xi \rightarrow \infty$ , we have  $\eta_k \rightarrow k\xi/\sqrt{2}$  and  $V_{23}^1 \rightarrow 2^{7/4} V_0 \xi^{-3/2}/3$ . The collisional integral now becomes

$$\begin{aligned} \text{St}_k &= \frac{32\sqrt{2}\pi^2 V_0^2}{9\xi^3 k} \int_{k_1, k_2 \geq 0} (\mathcal{T}_{12}^k \delta(\omega_{12}^k) - \mathcal{T}_{k_2}^1 \delta(\omega_{k_2}^1) \\ &- \mathcal{T}_{k_1}^2 \delta(\omega_{k_1}^2)) k_1 k_2 dk_1 dk_2. \quad (10) \end{aligned}$$

where now  $\omega_k = c\xi k^2/\sqrt{2}$ . Note that this collision integral coincides with the one for the finite- $k$  spectral part  $n'_k$  obtained from the four-wave kinetic equation via substitution  $n_k = N_0 \delta(\mathbf{k}) + n'_k$ ,  $N_0 = \text{const}$ ; see e.g. [15]. This fact is natural because both imply weak condensate, and the four-wave kinetic equation additionally assumes that the condensate's phase is random.

To find the Kolmogorov-type spectrum in the short-wave limit, we apply the standard procedure provided

by the WTT and seek a stationary power-law solution of (10),  $n_k = Ak^{-x}$ ,  $A = \text{const}$ . This leads to  $\text{St}_k = 64V_0^2\pi^2A^2(9\xi^4c_s)^{-1}k^{1-2x}I(x)$ , with the dimensionless collision integral

$$I(x) = \int_{q_1, q_2 \geq 0} (q_1 q_2)^{1-x} \left( (1 - q_1^x - q_2^x) \delta(1 - q_1^2 - q_2^2) - 2(q_1^x - 1 - q_2^x) \delta(q_1^2 - 1 - q_2^2) \right) dq_1 dq_2. \quad (11)$$

The energy flux is  $P(k) = \frac{128\sqrt{2}}{9}\pi^3V_0^2\xi^{-3}A^2\frac{I(x)}{2x-6}k^{6-2x}$ . Constant energy flux,  $P(k) \equiv P_0 = \text{const}$ , implies  $2x - 6 = 0$ , i.e.  $x = 3$  and  $I(3) = 0$ . Using L'Hôpital rule,  $\lim_{x \rightarrow 3} I(x)/(x-3) = dI(x)/dx|_{x=3}$ . In Appendix B, we evaluate this expression and find

$$E(k) = C_2 c_s^{1/2} \xi^{5/2} P_0^{1/2} k, \quad C_2 = 2^{3/4} / \sqrt{\pi(\pi - 4 \ln 2)}. \quad (12)$$

This spectrum, as well as the constant  $C_1$  in (9), are new theoretical predictions. Note that the constants  $C_1$  and  $C_2$  are finite because the respective integrals defining the energy flux are convergent – a property called locality of the wave interactions (see Appendix B). We will now test these predictions numerically via simulations of the GPE and the isotropic WKE.

We perform numerical simulations of the forced-dissipated GPE (2) using the standard massively-parallel pseudo-spectral code FROST [16] with a fourth-order Exponential Runge-Kutta temporal scheme (see [8, 17, 18]). In addition, the condensate amplitude (at  $k = 0$ ) is kept constant during the evolution. We set the initial data with uniform condensate with  $|\Psi(0)|^2 = \rho_0$ , the forcing then adds the wave disturbances, and we evolve the system until it reaches a steady state. We then perform averages over time. We use grids of  $N_p^3$  collocation points. We set density  $\rho_0 = 1$  and  $c_s = 1$ , and  $\xi = \theta \Delta x$  where the grid length  $\Delta x = L/N_p$  and  $L = 2\pi$ . The forcing term is supported on a narrow band ( $1 \leq k \leq 3$ ) and it obeys the Ornstein–Uhlenbeck process  $dF_{\mathbf{k}}(t) = -\gamma \widehat{\Psi}_{\mathbf{k}} dt + f_w dW_{\mathbf{k}}$  where  $W_{\mathbf{k}}$  is the Wiener process. The parameters  $\gamma$  and  $f_0$  control the correlation time and the amplitude of the forcing respectively. Dissipation is of the form  $D_{\mathbf{k}} = (k/k_R)^{2\alpha}$  acting at the small scales. Finally, the  $k$ -space energy fluxes  $P(k)$  are computed directly using the GPE (2) (see SM of [12]). We verify that the simulated WT is in a weakly nonlinear regime by measuring spatio-temporal spectra of  $\Psi(\mathbf{x}, t)$  and confirming that they are narrowly concentrated around the dispersion curve (1) (see Appendix C).

We simulate the isotropic WKE (7) and (8), using the code WavKinS [19]. We also include forcing and dissipation terms, similarly to the GPE. We use a logarithmic grid of  $N_r$  points spanning the spectral domain  $[k_{\min}, k_{\max}]$ . The collision integral is a 1D integral obtained by making explicit use of the parametrization of the resonant manifold provided in Appendix A. It is computed using the trapezoidal rule on the log-grid and a linear interpolation scheme. Time advancement is done

by the Runge-Kutta 2 method. Forcing is of the form  $f_k = f_0 k^s e^{-(k-k_f)^2/\Delta k_f^2}$  and dissipation  $-(k/k_d)^\beta n_k$ . Parameters are optimized to obtain a large inertial range, while resolving the spectrum well. See Appendix C for more details on our methods.

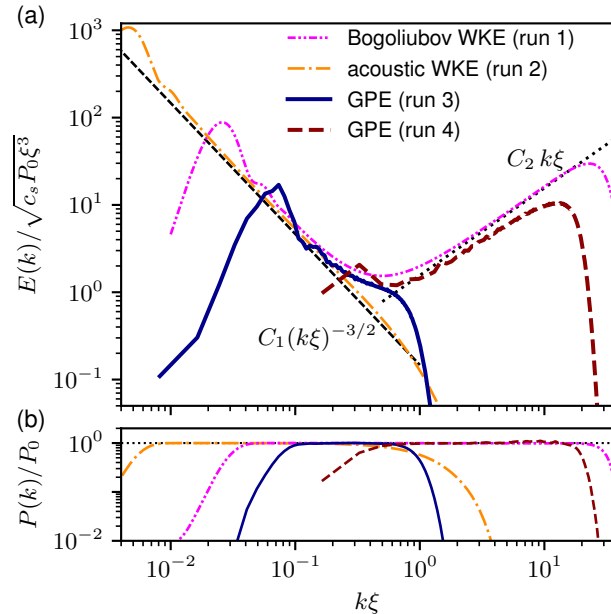


FIG. 1: Numerical results obtained by simulating WKE and GPE respectively. (a) Dimensionless energy spectra  $E(k)/\sqrt{c_s P_0 \xi^3}$  vs. dimensionless wave number  $k\xi$  with theoretical predictions (9) and (12) superimposed. (b) Corresponding energy fluxes normalized by their values measured in the inertial range.

We perform two isotropic WKE simulations: one of the Bogoliubov WKE (7) and the other one of the purely acoustic WKE (8). We also perform two GPE simulations with  $\theta = 1.25$  and  $\theta = 15$  to focus on different ranges concerning the transitional wave number  $k_\xi = 1/\xi$ . The results of these runs in terms of the energy spectra and the fluxes superimposed with the respective theoretical predictions (9) and (12) are presented in Fig 1. The energy fluxes shown in Fig 1(b) exhibit plateau ranges, with  $P(k) = P_0 = \text{const}$ , in which the spectra are stationary and both forcing and dissipation effects are negligible (the so-called inertial range). The measured values of  $P_0$  are then used for normalizing the energy spectra in Fig 1(a). We can see that each of the respective inertial ranges, for both WKE and GPE simulation, are in excellent agreement with our theoretical predictions (both in the spectral slopes and the prefactor constants). The longest inertial range, spanning for about two decades, is realized in the acoustic WKE run with scaling spectrum (9) confirmed. The Bogoliubov WKE run produced simultaneously two scaling ranges in the large-scale and the short-scale parts of the spectrum (about one decade wide each). The GPE runs with small

and big values of  $\xi$  produced one scaling each for  $k\xi < 1$  and  $k\xi > 1$ . The scaling range in the GPE run with  $\theta = 1.25$  is the narrowest among all the simulations, but its spectrum agrees with the Bogoliubov WKE simulation. In particular, it exhibits a bump at the high- $k$  part of the spectrum close to the transitional wave number,  $k \sim k_\xi$ . A similar bump was previously observed in GPE simulations of [20], and it was called a "dispersive bottleneck" since it is related to an increased wave dispersion in this region of scales.

Now we will use the short-wave solution (12) for interpreting the experimental results of Dogra et al. [9] on the far-from-equilibrium EoS. Dogra et al. analyzed the particle spectra (occupation number spectra)  $\tilde{n}_k$  measured in the direct cascade of BEC turbulence by fitting a scaling-law of  $k^{-3+\delta}$ , with  $\delta$  being a small adjustable parameter. Note that at small scales, our prediction (12) corresponds to a  $k^{-3}$ -wave-action spectrum (equivalent to the particle spectrum, in this case, up to a prefactor difference), which coincides, up to the log-correction, with the 4-wave prediction found in [8]. Such a coincidence makes both spectra good candidates for explaining the experimentally found EoS.

The direct cascade solution of the 4-wave WKE found in [17], recast in a dimensional form, reads

$$\tilde{n}_k = n_{4w} k^{-3} \log^{-\frac{1}{3}} \left( \frac{k}{k_f} \right), n_{4w} = C_{4w} \left( \frac{m^2 \epsilon}{\hbar^3 a_s^2} \right)^{1/3}, \quad (13)$$

where  $k_f$  is the forcing wave number and  $C_{4w} = C_d (4\pi)^{-\frac{2}{3}}$ , with  $C_d \approx 5.26 \times 10^{-2}$  an universal constant.  $m$  is the atom mass,  $\hbar$  is the reduced Planck constant, and  $a_s$  is the  $s$ -wave length. The energy flux  $\epsilon$  is defined as the energy per unit of volume dissipated in the system per unit time.

In Reference [9], the EoS is defined as the dependence of the non-dimensional spectrum amplitude,  $n_{4w}/N$  vs the non-dimensional energy flux  $\tilde{\epsilon} = m^2 \hbar^{-3} a_s^{-2} N^{-3} \epsilon$  where  $N$  is the mean particle density such that  $N = \int 4\pi k^2 \tilde{n}_k dk$  with the definition of  $\tilde{n}_k$  as in this paper. Theoretical prediction (13) implies  $n_{4w}/N = C_{4w} \tilde{\epsilon}^{1/3}$ , which was confirmed in [9] for data points with low values of  $\tilde{\epsilon}$ . However, at larger  $\tilde{\epsilon}$ , [9] reported a steeper EoS,  $n_{4w}/N \sim \tilde{\epsilon}^\alpha$  with  $\alpha > 1/3$ . The authors of [9] noted that  $\alpha \approx 2/3$  provide a good fit implying a flux-dependence like the one of the classical Kolmogorov hydrodynamic turbulence. However, it is unclear how a state with the classical Kolmogorov turbulence could appear in this experiment, considering that it is unlikely that the cascade process is generated by vortices with hydrodynamic properties. Indeed, such regimes are usually attributed to states with polarised vortex tangles at scales greater than the inter-vortex distance [21], which do not seem to be relevant to the considered experiment. Also, as noted in [9], the Kolmogorov spectrum would imply a spectral exponent that is different from the observed exponent  $\approx -3$ . Another point is that the EoS observed in [9] shows a dependence on the mean particle

density  $N$  that can not be explained by (13).

Here, we suggest a plausible interpretation of the steeper EoS and its dependence on  $N$ . We propose that a stronger ground-state condensate component could be present for greater  $\tilde{\epsilon}$  making the system to switch to the three-wave turbulence of short Bogoliubov waves, implying  $\alpha \approx 1/2 > 1/3$ .

Recasting our prediction (9) in the same manner as in (13), we obtain (see Appendix D for details)

$$\tilde{n}_k = n_{3w} k^{-3}, \frac{n_{3w}}{N} = C_{3w} \left( \frac{m^2 \epsilon}{\hbar^3 N^3 a_s^2} \right)^{1/2}, C_{3w} = \frac{C_2}{2^{17/4} \pi^2}. \quad (14)$$

The dimensional  $P_0$  in (9) is related to  $\epsilon$  as  $\epsilon = \rho_0 P_0$ , since  $P_0$  complies with the standard definition of the energy flux as the energy dissipation rate per unit mass whereas  $\epsilon$  used in [9] is the energy dissipation rate per unit volume. The EoS corresponding to (14) is  $n_{3w}/N = C_{3w} \tilde{\epsilon}^{1/2}$ .

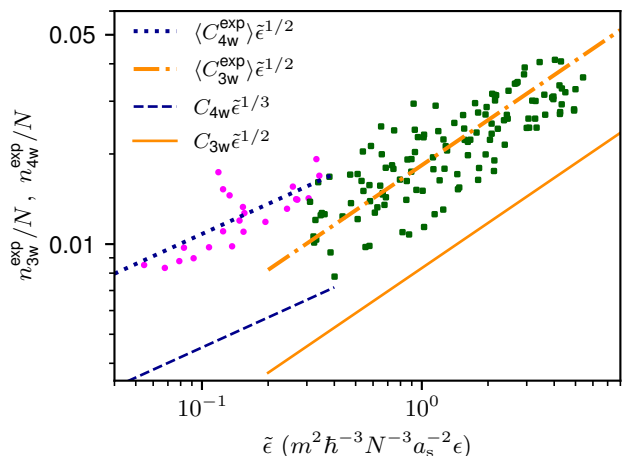


FIG. 2: EoS generated from the experimental data of [9]. Green and magenta points correspond to the spectra that are best fitted by the three-wave and the four-wave predictions respectively.

The revised EoS based on the experimental data points of [9] is shown in Fig. 2. In [9], the EoS is presented as a dependence  $n_0/N$  vs  $\tilde{\epsilon}$ , with  $n_0$  found from fitting the experimental spectra with  $\tilde{n}_k = n_0 k^{-3.2}$ . Our procedure is different: for each experimentally obtained spectrum, we fit our two theoretical predictions  $\tilde{n}_k = n_{4w}^{\text{exp}} k^{-3} \log^{-\frac{1}{3}} \left( \frac{k}{k_f} \right)$ , and  $\tilde{n}_k = n_{3w}^{\text{exp}} k^{-3}$ . We then select the spectrum amplitude to be either  $n_{4w}^{\text{exp}}$  or  $n_{3w}^{\text{exp}}$  depending on which one provides a better fit (see Appendix D). Figure 2 also shows the theoretical four-wave and three-wave EoS predictions in which the constants  $C_{4w}$  and  $C_{3w}$  are replaced by the mean values of the respective constants obtained by fits of the experimental spectra,  $\langle C_{4w}^{\text{exp}} \rangle$  and  $\langle C_{3w}^{\text{exp}} \rangle$ . We see that the theoretical predictions are consistent with the experimental data, with the four-wave and three-wave EoS in agreement with the low

and high  $\tilde{\epsilon}$  parts respectively. The mean experimental constants are nearly twice the theoretically predicted values,  $\langle C_{3w}^{\text{exp}} \rangle \approx 2.2C_{3w}$  and  $\langle C_{4w}^{\text{exp}} \rangle \approx 2.4C_{4w}$ . However, the spread of the EoS data points appears to be approximately the same,  $\Delta C_{4w} \approx 2.3C_{3w}$  and  $\Delta C_{4w} \approx 1.7C_{4w}$ , which are of a similar size to the spread of the experimental points. We conclude that our theoretical predictions agree with the experimental data within the measurement error bars.

In summary, in this Letter, we obtained the Kolmogorov-type stationary spectrum of forced-dissipated turbulence of short Bogoliubov waves, Eq.(12), and we revised the long-wave Kolmogorov-type spectrum including finding the exact prefactor constant  $C_1$ , see (9). We have validated these solutions, along with the combined spectrum including both long and short waves by numerical simulations of the GPE and the isotropic Bogoliubov WKE. We used the newly found short-wave spectrum for interpreting the (previously unexplained) experimental Equation of State of Ref.[9]. To test our theory in future experiments, the realizability of short Bogoliubov waves must be examined, namely (i) check if a strong ground state is present for strong forcing cases, (ii) check that for these cases the measured spectrum corresponds to waves shorter than the healing length and with amplitudes weaker than the ground state. Further, it would be interesting to study stronger waves whose statistics is not described by the WTT.

#### ACKNOWLEDGMENTS

This work was funded by the Simons Foundation Collaboration grant Wave Turbulence (Award ID 651471). This work was granted access to the high-performance computing facilities under GENCI (Grand Equipement National de Calcul Intensif) A0102A12494 (IDRIS and ADASTR), the OPAL infrastructure from Université Côte d'Azur, supported by the French government, through the UCAJEDI Investments in the Future project managed by the National Research Agency (ANR) under Reference No. ANR-15-IDEX-01.

# Turbulence and far-from-equilibrium equation of state of Bogoliubov waves in Bose-Einstein Condensates: Supplemental material

## Appendix A: Derivation of wave-kinetic equations

In this Supplemental Material, we first review the Hamiltonian formulation of Bogoliubov waves following the methods in [7, 12] to obtain the interaction term represented by  $V_{23}^1$  in Eq. (6). We also validate  $V_{23}^1$  by using the Bogoliubov transformation. The angular average of the Dirac- $\delta$  function in terms of wavevectors is discussed, which is essential to getting the isotropic WKE. Specifically, we clarify that even in non-dispersive 3D acoustic systems, the singularity of WKE is canceled by taking an angular average of  $\delta(\mathbf{k} - \mathbf{k}_1 - \mathbf{k}_2)$ , which results in a prefactor of the corresponding WKE that is different from the one obtained for the dispersive case in the limit of vanishing dispersion.

### 1. Hamiltonian formation and wave interaction amplitude $V_{23}^1$

The action for Bogoliubov waves (per unit of mass) is expressed in hydrodynamic variables it is given by

$$\mathcal{S} = \frac{1}{\rho_0 L^3} \int dt d^3x \left[ -\rho \dot{\phi} - \frac{\rho}{2} (\nabla \phi)^2 - \frac{c_s^2}{2\rho_0} (\rho - \rho_0)^2 - c_s^2 \xi^2 (\nabla \sqrt{\rho})^2 \right], \quad (\text{A1})$$

which corresponds to a compressible, isentropic, irrotational fluid [22] but with an extra quantum pressure term  $c_s^2 \xi^2 (\nabla \sqrt{\rho})^2$ .  $L$  is the length of the triply-periodic box on which the problem is defined.

Following the change of variables defined in the SM of [12], i.e.,  $\rho = \rho_0(1 + A)^2$  and  $p = 2(1 + A)\phi$ , and applying a similar procedure, we get the second- and the third-order terms of the Hamiltonian,

$$H_2 = \int \frac{d^3x}{L^3} \left[ \frac{1}{8} (\nabla p)^2 + 2c_s^2 A^2 + c_s^2 \xi^2 (\nabla A)^2 \right], \quad H_3 = \int \frac{d^3x}{L^3} \left[ 2c_s^2 A^3 - \frac{1}{4} p (\nabla p) \cdot (\nabla A) \right], \quad (\text{A2})$$

with the total Hamiltonian being  $H \approx H_2 + H_3$ . By defining the Fourier series as  $p(\mathbf{x}) = \sum_{\mathbf{k}} p_{\mathbf{k}} e^{i\mathbf{k}\cdot\mathbf{x}}$  and  $A(\mathbf{x}) = \sum_{\mathbf{k}} A_{\mathbf{k}} e^{i\mathbf{k}\cdot\mathbf{x}}$ ,  $H_2$  and  $H_3$  become:

$$H_2 = \sum_{\mathbf{k}} \frac{1}{8} k^2 |p_{\mathbf{k}}|^2 + 2\omega_k^2 k^{-2} |A_{\mathbf{k}}|^2, \quad H_3 = \sum_{1,2,3} 2c_s^2 A_1 A_2 A_3 \delta_{1,2,3} + \frac{1}{4} p_1 p_2 A_3 \mathbf{k}_2 \cdot \mathbf{k}_3 \delta_{1,2,3}, \quad (\text{A3})$$

where  $\omega_k = c_s k \sqrt{1 + (k\xi)^2/2}$  is the Bogoliubov dispersion relation, and  $\delta_{1,2,3}$  is 1 if  $\mathbf{k}_1 + \mathbf{k}_2 + \mathbf{k}_3 = 0$ , and 0 otherwise.

To write the Hamiltonian in the canonical form, we perform the following change of variables,

$$p_{\mathbf{k}} = i\sqrt{2}\omega_k^{1/2} k^{-1} (a_{\mathbf{k}} - a_{-\mathbf{k}}^*), \quad A_{\mathbf{k}} = (2\sqrt{2})^{-1} \omega_k^{-1/2} k (a_{\mathbf{k}} + a_{-\mathbf{k}}^*), \quad (\text{A4})$$

so that  $H_2 = \sum_{\mathbf{k}} \omega_k a_{\mathbf{k}} a_{\mathbf{k}}^*$  and  $i\dot{a}_{\mathbf{k}} = \frac{\partial H}{\partial a_{\mathbf{k}}^*}$  in the leading order. Using the resonance condition that  $\mathbf{k}_1 + \mathbf{k}_2 + \mathbf{k}_3 = 0$ ,  $H_3$  reduces to

$$H_3 = \sum_{1,2,3} \frac{1}{8\sqrt{2}} c_s^{-1} (\omega_1 \omega_2 \omega_3)^{1/2} \left[ \frac{3}{\eta_1 \eta_2 \eta_3} + (k_1 k_2 k_3)^{-1} \left( \frac{k_1^3}{\eta_1} - \frac{k_2^3}{\eta_2} - \frac{k_3^3}{\eta_3} \right) \right] (a_1 a_2^* a_3^* + \text{c.c.}) \delta_{2,3}^1 = \sum_{1,2,3} V_{2,3}^1 (a_1 a_2^* a_3^* + \text{c.c.}) \delta_{2,3}^1, \quad (\text{A5})$$

where  $\eta_i \equiv \eta(k_i) = \sqrt{1 + (k_i \xi)^2/2}$ ,  $\omega_i \equiv \omega(k_i)$  for  $i = 1, 2, 3$ , and  $\delta_{2,3}^1 = \delta_{-1,2,3}$ .

Equation (A5) gives the expression of  $V_{23}^1$  as in Eq. (6). Note that by using the following identity provided by the frequency resonance,

$$\frac{k_1^3}{\eta_1} - \frac{k_2^3}{\eta_2} - \frac{k_3^3}{\eta_3} = 2 \left( \frac{k_2}{\eta_2 \xi^2} + \frac{k_3}{\eta_3 \xi^2} - \frac{k_1}{\eta_1 \xi^2} \right), \quad (\text{A6})$$

we get an equivalent expression for  $V_{23}^1 = V_0 \sqrt{k_1 k_2 k_3} W_{23}^1$  with

$$W_{23}^1 = \frac{1}{2\sqrt{\eta_1 \eta_2 \eta_3}} + \frac{\sqrt{\eta_1 \eta_2 \eta_3}}{3\xi^2 k_1 k_2 k_3} \left( \frac{k_2}{\eta_2} + \frac{k_3}{\eta_3} - \frac{k_1}{\eta_1} \right). \quad (\text{A7})$$

The above expression is more convenient for the case  $k\xi \rightarrow \infty$  whereas Eq. (6) is better for the  $k\xi \rightarrow 0$  limit.

## 2. A different method to obtain the interaction coefficient: the Bogoliubov transformation

A different way to find the interaction coefficient  $V_{23}^1$  exploits the Bogoliubov transformation. The starting point is the Hamiltonian (per unit of mass) for the GPE in terms of  $\Psi$  and  $\rho$ . It reads

$$H = \frac{1}{L^3 \rho_0} \int \left( c_s^2 \xi^2 |\nabla \Psi|^2 + \frac{c_s^2}{2\rho_0} (\rho - \rho_0)^2 \right) d^3x. \quad (\text{A8})$$

Consider weak disturbances on the background of a strong coherent condensate,  $\Psi(\mathbf{x}, t) = \Psi_0(1 + \psi(\mathbf{x}, t))$ , such that  $|\Psi_0|^2 = \rho_0$ ,  $\langle \psi(\mathbf{x}, t) \rangle = 0$  and  $|\psi| \ll 1$ ; then the second and third order of  $H$  become

$$H_2 = \frac{1}{L^3} \int \left( c_s^2 \xi^2 |\nabla \psi|^2 + \frac{c_s^2}{2} (\psi + \psi^*)^2 \right) d^3x, \quad H_3 = \frac{1}{L^3} \int c_s^2 |\psi|^2 (\psi + \psi^*) d^3x. \quad (\text{A9})$$

Write  $\psi(\mathbf{x}) = \sum_{\mathbf{k}} \psi_{\mathbf{k}} e^{i\mathbf{k}\cdot\mathbf{x}}$ ;  $H_2$  and  $H_3$  become

$$H_2 = \sum_{\mathbf{k}} c_s^2 (1 + k^2 \xi^2) |\psi_{\mathbf{k}}|^2 + \frac{c_s^2}{2} (\psi_{\mathbf{k}} \psi_{-\mathbf{k}} + \psi_{\mathbf{k}}^* \psi_{-\mathbf{k}}^*), \quad H_3 = \sum_{1,2,3} c_s^2 \psi_{\mathbf{k}_1} \psi_{\mathbf{k}_2}^* \psi_{\mathbf{k}_3}^* \delta_{23}^1 + \text{c.c.} \quad (\text{A10})$$

To kill the non-diagonal terms in  $H_2$ , we perform the method described in [11] and find a canonical transformation as follows:

$$\psi_{\mathbf{k}} = \frac{1}{2} \sqrt{\frac{k\xi}{\sqrt{2}\eta_k}} \left[ \left( 1 + \frac{\sqrt{2}\eta_k}{k\xi} \right) b_{\mathbf{k}} + \left( 1 - \frac{\sqrt{2}\eta_k}{k\xi} \right) b_{-\mathbf{k}}^* \right], \quad (\text{A11})$$

and the inverse transformation

$$b_{\mathbf{k}} = \frac{1}{2} \sqrt{\frac{k\xi}{\sqrt{2}\eta_k}} \left[ \left( 1 + \frac{\sqrt{2}\eta_k}{k\xi} \right) \psi_{\mathbf{k}} + \left( 1 - \frac{\sqrt{2}\eta_k}{k\xi} \right) \psi_{-\mathbf{k}}^* \right]. \quad (\text{A12})$$

Note that  $b_{\mathbf{k}}$  is dimensionless and  $H_2 = \sum_{\mathbf{k}} \sqrt{2} c_s \xi \omega_k b_{\mathbf{k}} b_{\mathbf{k}}^*$ . Comparing to  $H_2 = \sum_{\mathbf{k}} \omega_k a_{\mathbf{k}} a_{\mathbf{k}}^*$ , one obtains the relation

$$b_{\mathbf{k}} = a_{\mathbf{k}} / \sqrt{\sqrt{2} c_s \xi}. \quad (\text{A13})$$

Now let us consider the  $H_3$  term. Under the canonical transformation (A11), after a long algebra, we get the following expression,

$$H_3 = \sum_{1,2,3} \frac{c_s^2}{4} \sqrt{\frac{k_1 k_2 k_3 \xi^2}{2\sqrt{2}\eta_1 \eta_2 \eta_3}} \left[ 3 + \frac{2\eta_1 \eta_2 \eta_3}{k_1 k_2 k_3} \left( \frac{k_2}{\eta_2 \xi^2} + \frac{k_3}{\eta_3 \xi^2} - \frac{k_1}{\eta_1 \xi^2} \right) \right] (b_{\mathbf{k}_1} b_{\mathbf{k}_2}^* b_{\mathbf{k}_3}^* + \text{c.c.}) \delta_{23}^1. \quad (\text{A14})$$

Substituting (A13) into the above equation, one gets the same expression as in the main text,  $V_{23}^1 = V_0 \sqrt{k_1 k_2 k_3} W_{23}^1$ , with  $W_{23}^1$  as in (A7).

The Bogoliubov transformation allows finding the relationship between the particle spectrum, defined as  $\tilde{n}_{\mathbf{k}} = \left(\frac{L}{2\pi}\right)^3 \langle |\Psi_{\mathbf{k}}|^2 \rangle / m = \left(\frac{L}{2\pi}\right)^3 \langle |\psi_{\mathbf{k}}|^2 \rangle \rho_0 / m$  (ignoring the zero mode), and the wave-action spectrum, defined as  $n_{\mathbf{k}} = \left(\frac{L}{2\pi}\right)^3 \langle |a_{\mathbf{k}}|^2 \rangle$ . In the acoustic limit,  $k\xi \rightarrow 0$ ,  $\psi_{\mathbf{k}} \rightarrow \frac{1}{\sqrt{2\sqrt{2}k\xi}} (b_{\mathbf{k}} - b_{-\mathbf{k}}^*) = \frac{1}{2\xi\sqrt{c_s k}} (a_{\mathbf{k}} - a_{-\mathbf{k}}^*)$ . Assuming that  $a_{\mathbf{k}}$  and  $a_{-\mathbf{k}}$  have the same amplitude and independent random phases (consistent with the so-called random amplitude and phases assumption in WWT plus the isotropy assumption), one gets that  $\langle |\psi_{\mathbf{k}}|^2 \rangle = \frac{1}{2\xi^2 c_s k} \langle |a_{\mathbf{k}}|^2 \rangle$  and consequently

$$\tilde{n}_{\mathbf{k}} = \frac{\rho_0}{2m\xi^2 c_s k} n_{\mathbf{k}}. \quad (\text{A15})$$

In the short-wave limit,  $k\xi \rightarrow \infty$ ,  $\eta_k \rightarrow k\xi/\sqrt{2}$ , we have  $\psi_{\mathbf{k}} \rightarrow b_{\mathbf{k}} = \frac{1}{\sqrt{\sqrt{2}c_s \xi}} a_{\mathbf{k}}$ , which results in

$$\tilde{n}_{\mathbf{k}} = \frac{\rho_0}{\sqrt{2}m c_s \xi} n_{\mathbf{k}}. \quad (\text{A16})$$

### 3. Angular average of $\delta(\mathbf{k} - \mathbf{k}_1 - \mathbf{k}_2)$

To get the isotropic WKE, we only need to compute the angular average of the Dirac- $\delta$  function of wavevectors in Eq. (5), since  $V_{23}^1$  and frequency are both angle-independent. Writing  $d\mathbf{k} = k^2 d\Omega dk$ , where  $d\Omega = \sin\theta d\theta d\phi$ , the angular average of  $\delta(\mathbf{k} - \mathbf{k}_1 - \mathbf{k}_2)$  is then defined as  $\Delta = \int \delta(\mathbf{k} - \mathbf{k}_1 - \mathbf{k}_2) d\Omega_1 d\Omega_2$ .

We define a coordinate system and the spherical angles as shown in Fig. S1(a). Decomposing  $\delta(\mathbf{k} - \mathbf{k}_1 - \mathbf{k}_2)$  in

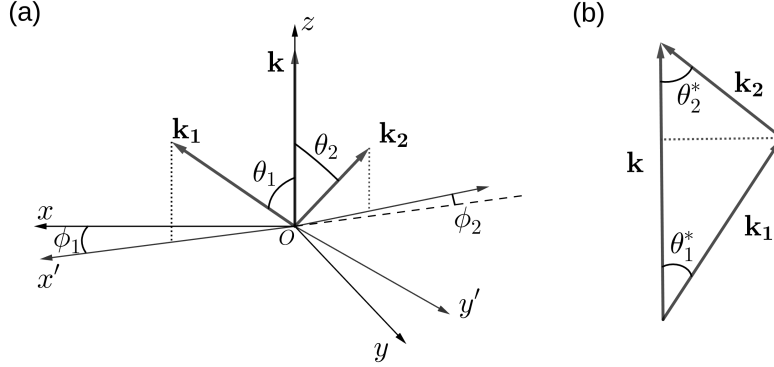


FIG. S1: (a) Coordinates system to compute  $\Delta$ ; (b) Wave vector triad.

these coordinates, we get

$$\begin{aligned} \Delta &= \int \delta(k_1 \sin \theta_1 + k_2 \sin \theta_2 \cos(\phi_2 + \pi)) \delta(k_2 \sin \theta_2 \sin(\phi_2 + \pi)) \delta(k - k_1 \cos \theta_1 - k_2 \cos \theta_2) \sin \theta_1 \sin \theta_2 d\theta_1 d\theta_2 d\phi_1 d\phi_2 \\ &= 2\pi \int \delta(k_1 \sin \theta_1 - k_2 \sin \theta_2 \cos \phi_2) \delta(k_2 \sin \theta_2 \sin \phi_2) \delta(k - k_1 \cos \theta_1 - k_2 \cos \theta_2) \sin \theta_1 \sin \theta_2 d\theta_1 d\theta_2 d\phi_2. \end{aligned} \quad (\text{A17})$$

It is easy to find that the system of equations  $h_1(\theta_1, \theta_2, \phi_2) \equiv k_1 \sin \theta_1 - k_2 \sin \theta_2 \cos \phi_2 = 0$ ,  $h_2(\theta_1, \theta_2, \phi_2) \equiv k_2 \sin \theta_2 \sin \phi_2 = 0$ , and  $h_3(\theta_1, \theta_2, \phi_2) \equiv k - k_1 \cos \theta_1 - k_2 \cos \theta_2 = 0$  has a unique solution  $\theta_1 = \theta_1^*$ ,  $\theta_2 = \theta_2^*$  and  $\phi_2 = 0$  for given  $k > 0$ ,  $k_1, k_2 \geq 0$ , in the range  $0 \leq \theta_1, \theta_2 \leq \pi$ , and  $0 \leq \phi_2 \leq 2\pi$ . Consequently, we obtain

$$\Delta = \frac{2\pi \sin \theta_1^* \sin \theta_2^*}{|\nabla(h_1, h_2, h_3)|_{(\theta_1^*, \theta_2^*, 0)}} = 2\pi \sin \theta_1^* \sin \theta_2^* / |k_1 k_2^2 \sin \theta_2^* (\cos \theta_2^* \sin \theta_1^* + \cos \theta_1^* \sin \theta_2^*)|. \quad (\text{A18})$$

Note that in the resonant triangle as shown in Fig. S1(b), we have  $k_2(\cos \theta_2^* + \cos \theta_1^* \sin \theta_2^* / \sin \theta_1^*) = k$  and we finally get

$$\Delta = \frac{2\pi}{kk_1 k_2}. \quad (\text{A19})$$

Note that for expression (A18) to be determined, the vectors  $\mathbf{k}, \mathbf{k}_1$  and  $\mathbf{k}_2$  cannot be strictly co-linear, as is the case for non-dispersive sound. Therefore, in this derivation, it is essential that the system is dispersive. Otherwise,  $\Delta$  is 0/0 undetermined, i.e. the above method originated from [13] fails, as was already stressed in [13].

Another way to compute  $\Delta$  is representing the Dirac- $\delta$  function as

$$\delta(\mathbf{k} - \mathbf{k}_1 - \mathbf{k}_2) = \frac{1}{(2\pi)^3} \int_{\mathcal{R}^3} \exp[-i\mathbf{r} \cdot (\mathbf{k} - \mathbf{k}_1 - \mathbf{k}_2)] d\mathbf{r}. \quad (\text{A20})$$

Now we rewrite  $\Delta = \frac{1}{4\pi} \int \delta(\mathbf{k} - \mathbf{k}_1 - \mathbf{k}_2) d\Omega d\Omega_1 d\Omega_2$ , and substitute (A20) into it. Following the method in [17] and using Mathematica, we obtain an analytical expression

$$\Delta = \pi (\text{sign}(k_1 + k_2 - k) + \text{sign}(k + k_1 - k_2) + \text{sign}(k + k_2 - k_1) - 1) / (kk_1 k_2). \quad (\text{A21})$$

Consider a resonant condition such that  $\mathbf{k}, \mathbf{k}_1$ , and  $\mathbf{k}_2$  form a non-degenerated triangle, then, one gets the same  $\Delta$  as (A19).

For the degenerate resonant manifold of non-dispersive sound waves, we have  $\mathbf{k} \parallel \mathbf{k}_1 \parallel \mathbf{k}_2$ ,  $\text{sign}(k_1 + k_2 - k) = 0$ , so we get

$$\Delta_{\text{nondisp}} = \frac{\pi}{kk_1k_2}. \quad (\text{A22})$$

Note that the previous term differs in a factor 2 with respect to Eq. A19 as a consequence of the discontinuous character of formula (A21).

Surprisingly, the non-dispersive isotropic WKE of acoustic turbulence in 3D is regular. However, in order to make sense to the WKE, in its derivation, one should take first the limit of large box, followed by the angle average, and finally the large time limit (small nonlinearity). The resulting isotropic 3D acoustic WKE has the same form as Eq. (8), except that the prefactor is now  $2\pi^2V_0^2/c_s$ .

#### 4. Parametrization of the resonant manifold of Bogoliubov waves

After angular average, the resonant manifold of the wave kinetic equation (7) takes a much simpler and compact form. Noting that the second and the third terms of the right hand side are the same after permutation of indexes, one is left with only two resonant manifolds determined by the following equations

$$h_1(k, k_1, k_2) \equiv \omega_1 + \omega_2 - \omega_k = 0, \quad h_2(k, k_1, k_2) \equiv -\omega_1 + \omega_2 + \omega_k = 0, \quad (\text{A23})$$

for the first and the second integral respectively. One can easily express  $k_2$  as a function of  $k$  and  $k_1$ , which for both equations reads

$$k_2^* = k_2(k, k_1) = \frac{1}{\xi} \left[ \sqrt{1 + \frac{2\xi^2}{c_s^2}(\omega_k - \omega_1)^2 - 1} \right]^{1/2}. \quad (\text{A24})$$

The above solution is valid for  $k_1 \leq k$  in the case  $h_1(k, k_1, k_2) = 0$ , and for  $k \leq k_1$  in the case  $h_2(k, k_1, k_2) = 0$ .

Finally, note that to evaluate the integrals of the WKE, one needs to compute

$$g(k_2) = \left| \frac{\partial h_1}{\partial k_2} \right| = \left| \frac{\partial h_2}{\partial k_2} \right| = c_s \frac{1 + \xi^2 k_2^2}{\sqrt{1 + \frac{1}{2}\xi^2 k_2^2}}, \quad (\text{A25})$$

which is always positive, and therefore, no singularities are present in the Bogoliubov WKE.

Using the previous two equations, we can express the Bogoliubov WKE in an explicit form

$$\frac{\partial n_k}{\partial t} = \frac{4\pi^2 V_0^2}{c_s} \left[ \int_0^k |W_{12^*}^k|^2 \frac{k_1^2 k_2^{*2}}{g(k_2^*)} \mathcal{T}_{12^*}^k dk_1 - 2 \int_k^\infty |W_{k2^*}^1|^2 \frac{k_1^2 k_2^{*2}}{g(k_2^*)} \mathcal{T}_{k2^*}^1 dk_1 \right], \quad (\text{A26})$$

where we recall that  $\mathcal{T}_{12}^k = n_{k_1} n_{k_2} - n_k n_{k_1} - n_k n_{k_2}$ , and that  $k_2^*$  is given by Eq. (A24).

### Appendix B: Derivation of Kolmogorov-type spectra

In this section, we derive the stationary Kolmogorov-type spectra for the acoustic and short-wave limits, including convergence analysis of the collision integral and calculation of constants.

#### 1. Zakharov-Sagdeev spectrum

Seeking a power-law solution in the form of  $n_k = Ak^{-x}$ , and substituting it into Eq. (8), the right hand side becomes  $\text{St}_k = 4\pi^2 V_0^2 c_s^{-1} A^2 k^{5-2x} I(x)$  with the dimensionless collision integral

$$I(x) = \int_{q_1, q_2 \geq 0} (q_1 q_2)^{2-x} ((1 - q_1^x - q_2^x) \delta(1 - q_1 - q_2) - (q_1^x - q_2^x - 1) \delta(q_1 - q_2 - 1) - (q_2^x - q_1^x - 1) \delta(q_2 - q_1 - 1)) dq_1 dq_2. \quad (\text{B1})$$

Therefore the energy flux  $P(k) = -\int_0^k 4\pi \tilde{k}^2 \omega(\tilde{k}) \text{St}(\tilde{k}) d\tilde{k}$  becomes  $P(k) = 16\pi^3 V_0^2 A^2 \frac{I(x)}{2x-9} k^{9-2x}$ . The stationarity of the spectrum means constant flux  $P = P_0$  — independent on  $k$ , which suggests that  $x = 9/2$  and  $I(9/2) = 0$ . In such case, one gets  $P_0 = 8\pi^3 V_0^2 A^2 I'(9/2)$  by using the L'Hôpital rule, where  $I'(9/2) = dI(x)/dx|_{x=9/2}$ . Consequently we have the stationary spectrum  $n_k = \sqrt{P_0/(8\pi^3 V_0^2 I'(9/2))} k^{-9/2}$  and  $E(k) = 4\pi c_s \sqrt{P_0/(8\pi^3 V_0^2 I'(9/2))} k^{-3/2}$ .

To obtain the constant, we need to: 1) check if  $I(x)$  is convergent and differentiable at  $x = 9/2$ : this is called the locality property; 2) prove that  $I(9/2) = 0$  and compute  $I'(9/2)$ . For this purpose, we rewrite the collision integral as

$$I(x) = 2 \left( \int_0^{1/2} (f_1(q, x) - f_2(q, x)) dq - \int_{1/2}^{\infty} f_2(q, x) dq \right), \quad (\text{B2})$$

where  $f_1(q, x) = (q(1-q))^{2-x} (1-q^x - (1-q)^x)$  and  $f_2(q, x) = (q(1+q))^{2-x} ((1+q)^x - q^x - 1)$ . Note that  $f_1(q, x) - f_2(q, x) \propto q^{4-x}$  when  $q \rightarrow 0$  and  $f_2(q, x) \propto q^{3-x}$  when  $q \rightarrow \infty$ , which give us a convergence interval for  $I(x)$ , namely  $4 < x < 5$ .  $I(x)$  is also convergent at  $x = 1$  with  $I(1) = 0$  that corresponds to the thermal equilibrium solution.

Thanks to Mathematica, within the window of convergence we get

$$I(x) = 2^{2x-5} {}_2\tilde{F}_1(x-2, 2x-5; 2(x-2); -2)\Gamma(2x-5) + \frac{4}{(x-5)(x-4)(x-3)} + \frac{1}{2} B(3-x, 3-x) - (-1)^x B_{-\frac{1}{2}}(3-x, 3-x). \quad (\text{B3})$$

In Fig. S2(a) we plot  $I(x)$  in the convergence range. One can confirm that  $I(9/2) = 0$  by (B3).

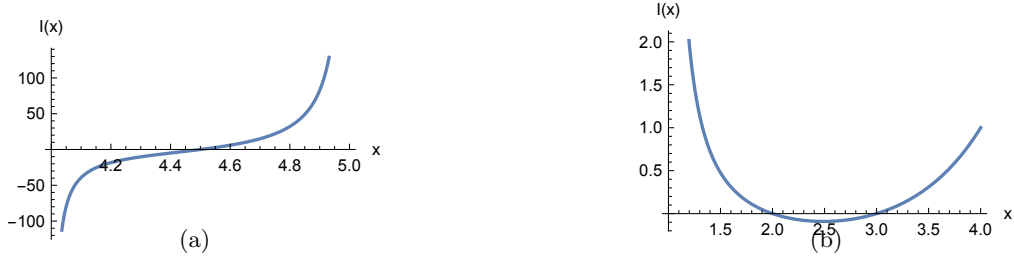


FIG. S2: Collision integrals in their convergence windows:  $I(x)$  is given by Eq. (B3) in (a) and by Eq. (B7) in (b).

Similarly, the derivative  $I'(9/2)$  is computed by

$$I'(9/2) = 2 \left( \int_0^{1/2} (f'_1(q, 9/2) - f'_2(q, 9/2)) dq - \int_{1/2}^{\infty} f'_2(q, 9/2) dq \right), \quad (\text{B4})$$

and we get  $I'(9/2) = 64(4 \ln 2 + \pi - 1)/3$ . Finally, we obtain the ZS spectrum with the constant as in Eq. (9).

Now let us consider the non-dispersive case, for which we have  $P(k) = 8\pi^3 V_0^2 A^2 \frac{I(x)}{2x-9} k^{9-2x}$ . Following the same procedure as above, we obtain

$$C_{1, \text{nondisp}} = \frac{\sqrt{2}}{\sqrt{3\pi(4 \ln 2 + \pi - 1)}}. \quad (\text{B5})$$

In [14], the constant observed for the non-dispersive acoustic system is smaller than the one for the dispersive system, unlike what we get here. Their paper offers an explanation based on a numerical observation of an anisotropy (i.e. presumably the isotropic spectrum is unstable with respect to anisotropic perturbations). Note, however, that the model acoustic-wave equation studied in [14] was different from the compressible Euler equation or GPE. Thus, the question about the acoustic wave spectrum arising in the non-dispersive Euler equation merits further study.

## 2. Kolmogov-Zakharov spectrum for short Bogoliubov waves

For short waves, similarly to the procedure performed on acoustic waves, we study the convergence of the integral of Eq. (11) and compute the derivative  $I'(3)$ . We rewrite the collision integral as

$$I(x) = \int_0^1 g_1(q, x) dq - 2 \int_0^{\infty} g_2(q, x) dq, \quad (\text{B6})$$

where  $g_1(q, x) = \frac{1}{2}q^{1-x}(1-q^2)^{-x/2}(1 - q^x - (1 - q^2)^{-x/2})$ , and  $g_2(q, x) = \frac{1}{2}q^{1-x}(1+q^2)^{-x/2}((1 + q^2)^{-x/2}1 - q^x - 1)$ .

Note that  $g_1(q, x), g_2(q, x) \propto q^{3-x}$  when  $q \rightarrow 0$ , and  $g_2(q, x) \propto q^{1-2x}$  when  $q \rightarrow \infty$ , we find that  $I(x)$  is convergent for  $1 < x < 4$ . Using Mathematica, we get the analytical result:

$$I(x) = \frac{2}{x-2} - \frac{\sqrt{\pi}2^{x-3}(\sec(\frac{\pi x}{2}) - 1)\Gamma(1 - \frac{x}{2})}{\Gamma(\frac{3}{2} - \frac{x}{2})}, \quad (\text{B7})$$

and plot it in Fig. S2(b). With (B7), one can easily confirm that  $I(3) = 0$ , and find another solution  $x = 2$  that corresponds to the thermal equilibrium spectrum.

The derivative  $I'(3)$  then becomes  $I'(3) = \int_0^1 g_1'(q, 3) dq - 2 \int_0^\infty g_2'(q, 3) dq = \pi - 4\sqrt{2}$ . Finally, one gets the KZ spectrum for the short Bogoliubov waves, as in Eq. (12).

## Appendix C: Details on numerical simulations

### 1. Numerical simulations of the wave kinetic equation

We integrate the WKE (A26) using the code WavKinS [19]. The code uses a logarithmic mesh  $\{k_i = C\lambda^i, i = 1, \dots, N_r\}$ , where  $\lambda$  is chosen in order to span the integration domain  $[k_{\min}, k_{\max}]$ . Intermesh values are obtained using a linear interpolation that ensures positivity. Integrals are performed using the trapezoidal rule, after performing a change of variable in the following manner

$$\int_{k_i}^{k_{i+1}} G(p) dp = \log \lambda \int_i^{i+1} G(\lambda^x) \lambda^x dx \approx \frac{\log \lambda}{2} (G(k_{i+1})k_{i+1} + G(k_i)k_i). \quad (\text{C1})$$

For the integral over the first bin, we make the following approximation  $\int_0^{k_1} G(p) dp \approx k_1 G(k_1)$ . Finally, we use a Runge-Kutta-2 time marching method, with a implicit scheme for the dissipative term.

### 2. Numerical parameters

All essential numerical parameters for the WKE and GPE runs are given in Table S1.

run	model	$N_r$	$k_{\min}$	$k_{\max}$	$f_0$	$n_d$	$s$	$k_f$	$\Delta k_f$	$\beta$	$k_d$
1	Bogoliubov WKE	32768	$1 \times 10^{-2}/\xi$	$200/\xi$	$1.032 \times 10^{14}$	6	4	0	$1.5 \times 10^{-2}$	1	80
2	acoustic WKE	8196	$1 \times 10^{-4}$	1	$2.419 \times 10^{16}$	2	2	0.01	0.028	1	0.6

run	model	$N_p$	$\alpha$	$f_w^2$	$\gamma$	$k_R$	$\xi$
3	GPE	960	3	$10^{-9}$	-1	260	$1.25\Delta x$
4	GPE	576	4	$10^{-4}$	-1	300	$15\Delta x$

TABLE S1: Parameters for GPE and WKE simulations.

### 3. Verifying the assumptions of the Wave Turbulence theory for the GPE simulations

To check if the WTT assumptions apply to the GPE simulations, we compute the normalized spatio-temporal spectral density  $S(\omega, k) \propto |\hat{\Psi}(k, \omega)|^2$ , where  $\hat{\Psi}(k, \omega)$  is the time and space Fourier transform of  $\Psi(\mathbf{x}, t)$ , averaged on the sphere  $|\mathbf{k}| = k$ . We present the spatio-temporal spectra in Fig. S3 (a) for GPE run 3 and (b) for run 4. Fig. S3 (a) demonstrates that for run 3, most of the spectrum is concentrated near the Bogoliubov dispersion  $\omega_{\text{Bogol}}(k) = c_s k \sqrt{1 + k^2 \xi^2 / 2}$ , which coincides with the dispersion relation of acoustic waves  $\omega_{\text{sound}}(k) = c_s k$  for  $k\xi < 0.5$ . For the short-wave simulation run 4, Fig. S3 (b) indicates that most waves concentrate around  $\omega_{\text{short}}(k) = c_s \xi k^2 / \sqrt{2}$ .

The nonlinearity of the systems is estimated by measuring the frequency broadening  $\delta\omega(k)$  around  $\tilde{\omega}(k)$  such that  $S(\omega, k)$  gets its maximum value for each fixed  $k$ . We plot the frequency broadening of run 3 and run 4 in

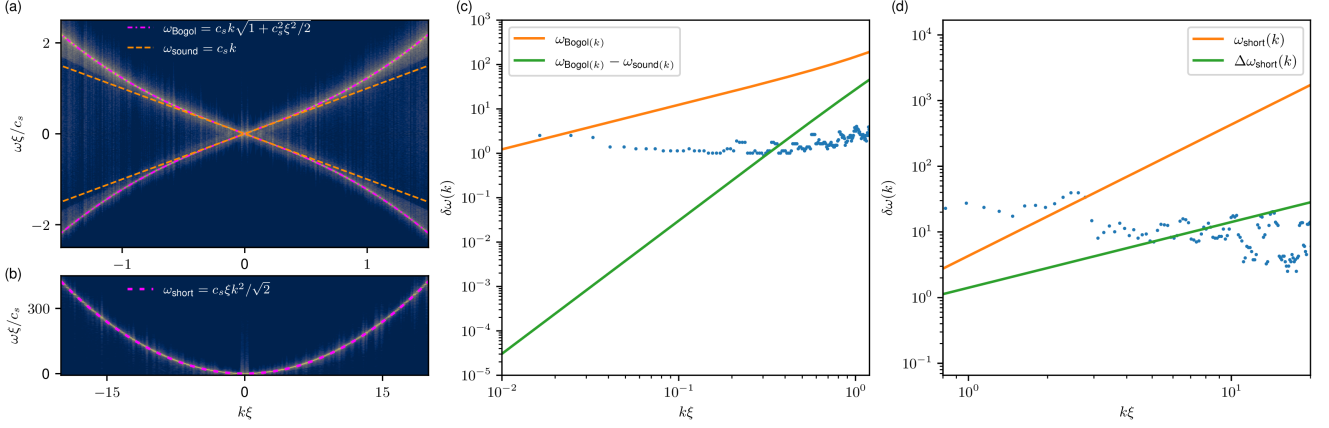


FIG. S3: Normalized spatio-temporal spectral density of  $\Psi(\mathbf{x}, t)$  for the GPE simulations of (a) run 3, and (b) run 4; Frequency broadening  $\delta\omega(k)$  (blue points) extracted from the corresponding spatial-temporal density spectra for (c) run 3, and (d) run 4.

Fig. S3(c) and (d), respectively. The WWT theory requires that: 1) The linear frequency is much bigger than nonlinear frequency broadening,  $\omega_{\text{Bogol}}(k) > \delta\omega(k)$ ; 2) A stronger requirement for the weakly-dispersive waves [11]: the dispersion correction to non-dispersive frequency,  $\omega_{\text{disp}}(k) = c_s k(\sqrt{1 + k^2 \xi^2/2} - 1)$ , is greater than  $\delta\omega(k)$ ; 3) To trigger the interactions, the nonlinear broadening must be greater than the spacing between the eigenmodes of the periodic box,  $\delta\omega(k) > \Delta\omega_{\text{Bogol}}(k)$ , where  $\Delta\omega_{\text{Bogol}}(k) = \Delta k d\omega_{\text{Bogol}}(k)/dk$  and  $\Delta k = 2\pi/L$  is the  $k$ -grid spacing. According to Fig. S3(c),  $0.2 < k\xi < 1$  meets the three conditions and it is also the range where the energy spectrum obtained by GPE run 3 agrees well with the one obtained by WKE run 1, as shown in Fig. 1. As noted, [14] obtained ZS spectrum in non-dispersive acoustic waves, which means condition 2) might not be necessary (this complicated issue is far from being settled). WWT for short waves requires that  $\omega_{\text{short}}(k) > \delta\omega(k)$  and  $\delta\omega(k) > \Delta\omega_{\text{short}}(k)$ , where  $\Delta\omega_{\text{short}}(k) = \Delta k d\omega_{\text{short}}(k)/dk$ . The  $k\xi$ -range that satisfies the two constraints of WTT, as shown in Fig. S3(d), are 2-15 for run 4. This range is consistent with the one where expected KZ spectra are observed in the main text. Details on how the normalized spatio-temporal spectral density and frequency broadening are calculated can be found in [17].

## Appendix D: Details on EoS

### 1. Equation of state for the 4-wave regime

In reference [8], the constant energy flux solution in the 4-wave regime was derived analytically and confirmed numerically. Its log-corrected spectrum reads

$$\tilde{n}_k = C_d (\epsilon \hbar / g^2)^{1/3} k^{-3} \ln^{-1/3}(k/k_f). \quad (\text{D1})$$

Substituting  $g = 4\pi \hbar^2 a_s / m$  into the above equation, one gets the equation of states of Eq. (13).

### 2. Equation of state for the 3-wave regime

We recall the relationship between the particle spectrum and the wave-action spectrum for short Bogoliubov waves (A16), and substitute  $n_k = \frac{E(k)}{4\pi k^2 \omega_{\text{short}}(k)}$ , the KZ solution Eq. (12), and  $P_0 = \epsilon / \rho_0$  into it. This gives

$$\tilde{n}_k = \frac{C_2 \rho_0^{1/2} \xi^{1/2}}{4\pi m c_s^{3/2}} \epsilon^{1/2} k^{-3}. \quad (\text{D2})$$

Then we express the parameters  $c_s$ ,  $\xi$  and  $\rho_0$  in terms of  $\hbar$ ,  $m$ ,  $a_s$  and  $N$  by the definitions  $\xi = \sqrt{\frac{\hbar^2}{2g\rho_0}}$ ,  $c_s = \sqrt{\frac{g\rho_0}{m^2}}$ ,  $g = 4\pi\hbar^2 a_s/m$ , and  $\rho_0 = mN$ . Finally, one gets

$$\tilde{n}_k = \frac{C_2}{2^{17/4}\pi^2} \frac{m\epsilon^{1/2}}{\hbar^{3/2}N^{1/2}a_s}, \quad (\text{D3})$$

and consequently the EoS Eq. 14.

### 3. Method to generate Fig. 2

For each  $\tilde{n}_k$  obtained by the experiment, we investigate the compensated spectra  $\tilde{n}_k k^3 \log^{1/3}(\frac{k}{k_f})$  and  $\tilde{n}_k k^3$ , respectively, and compute  $n_{4w}^{\text{exp}}$  and  $n_{3w}^{\text{exp}}$  by averaging the corresponding compensated spectrum in their plateau ranges.

To be consistent with theoretical predictions, one should note that we define the particle spectrum so that  $N = \int 4\pi k^2 \tilde{n}_k dk$ , where  $N$  is the mean particle density. A different convention was used in [9]: the particle spectrum was defined in the way that  $N = \frac{1}{(2\pi)^3} \int 4\pi k^2 \tilde{n}_k dk$ . This difference of notation has to be accounted for when comparing the results.

- 
- [1] S. Nazarenko, *Wave turbulence*, Vol. 825 (Springer Science & Business Media, 2011).
  - [2] S. Galtier and S. V. Nazarenko, *Physical review letters* **119**, 221101 (2017).
  - [3] V. S. L'vov and S. Nazarenko, *Low Temperature Physics* **36**, 785 (2010).
  - [4] P. Caillol and V. Zeitlin, *Dynamics of Atmospheres and Oceans* **32**, 81 (2000).
  - [5] S. Galtier, *Physical Review E* **68**, 015301 (2003).
  - [6] V. E. Zakharov, *Soviet Physics-JETP* **35**, 908 (1972).
  - [7] S. Dyachenko, A. Newell, A. Pushkarev, and V. Zakharov, *Physica D: Nonlinear Phenomena* **57**, 96 (1992).
  - [8] Y. Zhu, B. Semisalov, G. Krstulovic, and S. Nazarenko, *Physical Review Letters* **130**, 133001 (2023).
  - [9] L. H. Dogra, G. Martirosyan, T. A. Hilker, J. A. Glidden, J. Etrych, A. Cao, C. Eigen, R. P. Smith, and Z. Hadzibabic, *Nature* **620**, 521 (2023).
  - [10] G. Martirosyan, K. Fujimoto, and N. Navon, "An equation of state for turbulence in the gross-pitaevskii model," (2024), arXiv:2407.08738 [cond-mat.quant-gas].
  - [11] V. E. Zakharov, V. S. L'vov, and G. Falkovich, *Springer Series in Nonlinear Dynamics* (1992).
  - [12] A. Griffin, G. Krstulovic, V. S. L'vov, and S. Nazarenko, *Physical Review Letters* **128**, 224501 (2022).
  - [13] V. E. Zakharov and R. Z. Sagdeev, in *Doklady Akademii Nauk*, Vol. 192 (Russian Academy of Sciences, 1970) pp. 297–300.
  - [14] E. Kochurin and E. Kuznetsov, arXiv preprint arXiv:2407.08352 (2024).
  - [15] G. Düring, A. Picozzi, and S. Rica, *Physica D Nonlinear Phenomena* **238**, 1524 (2009).
  - [16] G. Krstulovic, *A theoretical description of vortex dynamics in superfluids. Kelvin waves, reconnections and particle-vortex interaction*, Habilitation à diriger des recherches, Université Côte d'Azur (2020).
  - [17] Y. Zhu, B. Semisalov, G. Krstulovic, and S. Nazarenko, *Physical Review E* **106**, 014205 (2022).
  - [18] Y. Zhu, B. Semisalov, G. Krstulovic, and S. Nazarenko, *Physical Review E* **108**, 064207 (2023).
  - [19] G. Krstulovic and V. Labarre, "Wavkins: Wave kinetic solver," (2024), currently under development.
  - [20] G. Krstulovic and M. Brachet, *Phys. Rev. Lett.* **106**, 115303 (2011).
  - [21] J. I. Polanco, N. P. Müller, and G. Krstulovic, **12**, 7090.
  - [22] L. Landau and E. Lifshitz, *Fluid Mechanics: Volume 6*, Vol. 6 (Elsevier, 1987).